Supplementary Information

Investigating the Morphological Transitions in an Associative Surfactant Ternary System

Houman Honaryar[1], *Jacob A. LaNasa*[2], *Robert J. Hickey*[2,3], *Julian C. Shillcock*[4,5], *Zahra Niroobakhsh*[1]*

[1] Department of Civil & Mechanical Engineering, University of Missouri-Kansas City, Kansas City, Missouri 64110, USA.
[2] Department of Materials Science & Engineering Pennsylvania State University, University Park, Pennsylvania 16802, USA.
[3] Materials Research Institute Pennsylvania State University, University Park, Pennsylvania 16802, USA.
[4] Laboratory of Molecular and Chemical Biology of Neurodegeneration, École polytechnique fédérale de Lausanne (EPFL), CH-1015 Lausanne, Switzerland.
[5] Blue Brain Project, École polytechnique fédérale de Lausanne (EPFL), Campus Biotech, Geneva 1202, Switzerland.
* Correspondence: niroobakhshz@umkc.edu

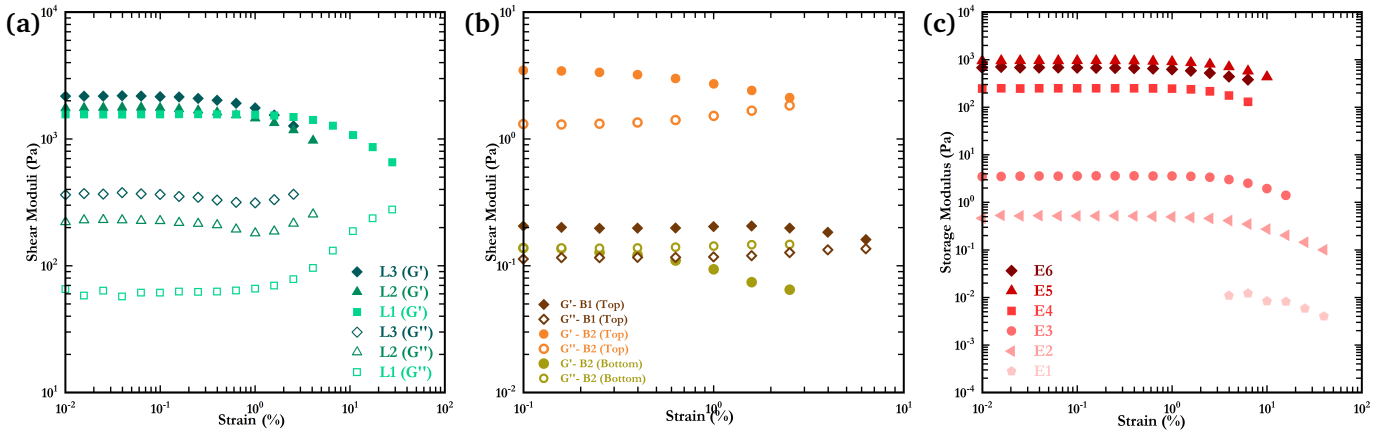

Figure S1 (a) Amplitude sweep curves for samples with constant CPCl concentration (425 mM) and varying OA content within L_α region (II). (b) amplitude sweep curves for two samples ("B1" and "B2") in L_1/L_α biphasic region (III). For sample "B2", amplitude sweep curves show that the shear moduli of the top phase is more than one order of magnitude higher than those of the bottom phase. Furthermore, the bottom phase of this sample ("B2") yields almost equal storage and loss moduli over the measured shear strain range. (c) Amplitude sweep curves for samples with equimolar ratio of CPCl and OA within L_α region (shown in Figure 9).

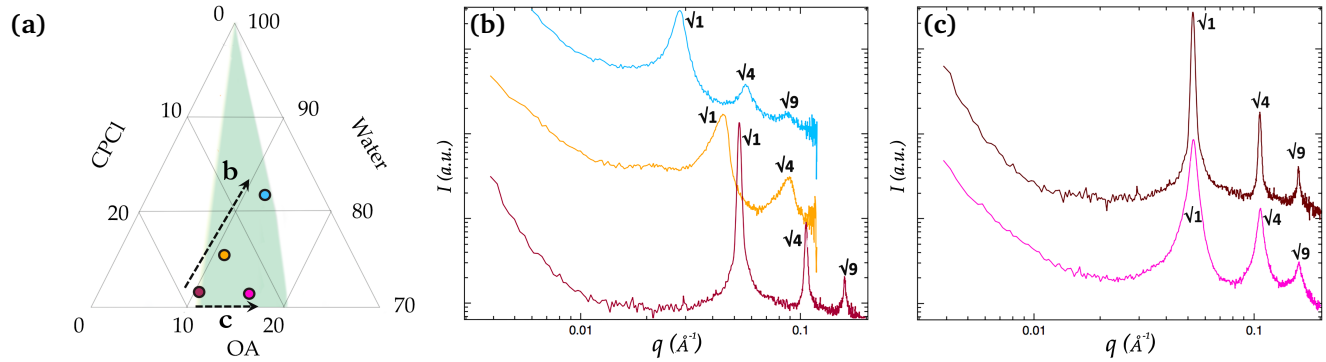

Figure S2 Effect of OA and water on domain spacing of L_α phase. (a) Composition of three samples at constant $wt\%_{OA}/wt\%_{water}$ (indicated along arrow "b") and two samples with constant water content (indicated along arrow "c") in region II of the ternary phase diagram, and their corresponding scattering patterns, shown in (b) and (c), respectively. The compositions in the ternary phase diagram are expressed in terms of weight percent.

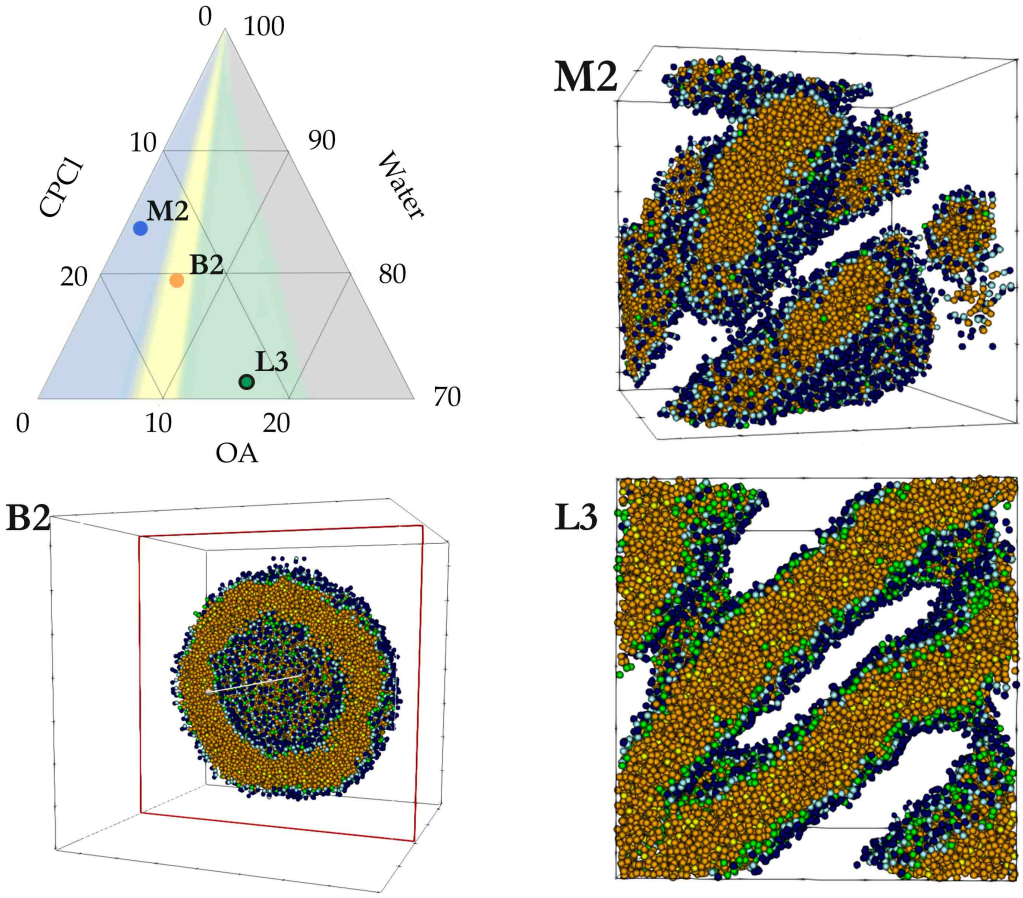

Figure S3 Formation of microstructure for three compositions (one in each region) when DPD conservative force parameters which quantify the interaction between headgroups OA and CPCl ($\varepsilon = a_{MH}, a_{NH}$) is reduced from 25 to 15. These snapshots show microstructures similar to the ones observed in Figure 10 where these force parameters (ε) are set to 25. The compositions in the ternary phase diagram are expressed in terms of weight percent.

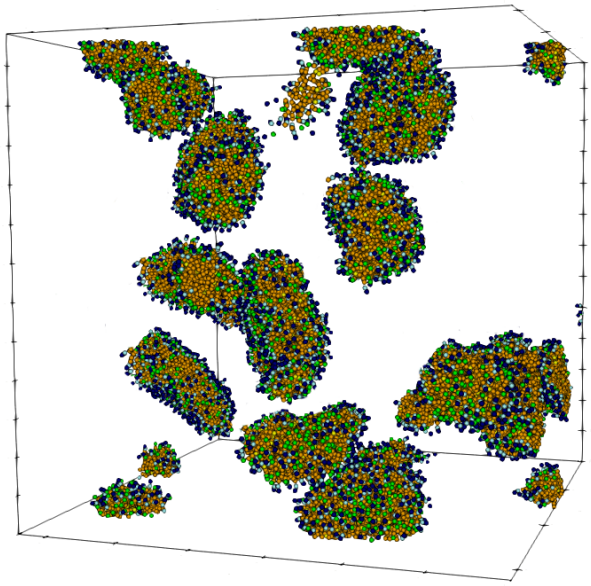

Figure S4 Micellar structure observed for composition "E1" (on the OA/CPCl equimolar line) in the large simulation box of $(64d_0)^3$.

Movie Legends

Playback speed of all movies are increased four times.

Movie S1 Evolution of the micellar structure of sample "M4" located in the micellar region (I) of the ternary phase diagram (Figure 12 diagram).

Movie S2 Evolution of the lamellar structure of sample "L1 (E5)" located in the lamellar/vesicle region (II) of the ternary phase diagram (Figures 9-11 diagram).

Movie S3 Evolution of the lamellar structure of sample "L2" located in the lamellar/vesicle region (II) of the ternary phase diagram (Figures 10-11 diagram).

Movie S4 Evolution of the lamellar structure of sample L3" located in the lamellar/vesicle region (II) of the ternary phase diagram (Figures 10-12 diagram).

Movie S5 Evolution of the vesicle for sample "B2" located in the L_1/L_α biphasic region (III) of the ternary phase diagram (Figures 10-12 diagram).